Lasercraft Dynamics and Design for Proxima Centauri b Flyby

Team 158

Problem A

Abstract

This paper analyses the combinations among various kinds of sail shapes, materials and laser beam shapes to be used in a laser propelled spacecraft meant to reach relativistic speeds. It is an attempt to find the best possible configuration for sending a probe on a flyby mission to the exoplanet Proxima Centauri b.

The best configuration is taken to be one that allows for stability, directional precision and maximum speed for a given mass.

An attempt to explain the dynamics of the sail and its underlying physics has been made. Analysis of the motion through the parameter space has been done to determine the possibility of a successful mission. Various parameters have been identified and different iterations of combinations of them have been considered. We have tried to optimize these parameters under the constraints of the problem statement so that our spacecraft may reach high enough speeds required for interstellar travel.

In terms of stability, disregarding power efficiency and material limitations, a spherical sail with a multimodal Gaussian beam appears to be the best option. However, we conduct an analysis of dynamics using a uniform beam, with the square sail performing best in this limited comparison. We also attempt to make estimations about the kind of error that would be permitted in the laser beam precision arriving at a value of the order of 10^{-10} radians.

Contents

1   Introduction

Breakthrough Starshot is a project with an aim to send an ultra-light nanocraft consisting of a space probe attached to a light sail of only a few grams, accelerated using the thrust of high power lasers for 10-20 minutes to achieve relativistic speeds, to the Alpha Centauri star system.

The laser array required for this endeavour has an output of of 50 GW. Because of the recoil generated due to this power, the laser array is taken to be ground based. An initial sailcraft displacement of 60 000 km is used, consistent with a low-thrust non Keplerian orbit that keeps the sailcraft (and associated spacecraft) stationary in the sky relative to the target. [4]

The flyby, required here, is to the planet Proxima Centauri b at a minimum distance not more than the distance between Earth and Moon. Additionally, a lightsail of an area of 10 square meters has been prescribed for this purpose.

A highly reflecting sail is required for efficient generation of thrust. At the mandated goal of near 20% of the speed of light, the nanocraft heats up rapidly. Thus, the sail also has to be of a material that can easily radiate in the range of mid-infrared while reflecting the incident laser.

The sail shape and laser wavefront combination has to be self-stabilizing, with a high degree of precision required in laser directionality.

2   Notations used

Symbol	Meaning	Numerical Value
d	length of side of laser array	10 km
D	diameter of reflector	3.16 m
m	mass of lightsail	2 g
λ	wavelength of laser	1064 nm
c	speed of light	3×10^8 ms^{-1}
P_o	power of laser array	50 GW
L_o	distance at which laser spot size equals sail size	
β	ratio of velocity of sail to c	
γ	$1/(1-\beta^2)^{0.5}$	

3 Laser Array Specifications

As proposed by Lubin [1], a full scale DE-STAR 4 phase locked laser array that is 10km along one side is proposed using Nd:YAG lasers with wavelength 1064 nm. This wavelength allows for minimal deviation by atmospheric disturbances. In certain cases discussed below we shall also look at a circular laser array having the same power output and a diameter of 10km. Various sail shapes are discussed for these two laser array configurations. Additionally, the laser array can be configured to produce several varying types of beams including a uniform 'top-hat' beam, a Gaussian beam, or a multimodal beam designed for a particular sail shape.

Discussion on this uniformity of cross-section of the beam is necessarily interwoven with the choice of sail shape for optimization and is discussed with the same. Divergence θ is seen to be

$$\theta = \frac{\alpha \lambda}{d} \tag{1}$$

Here $\alpha = 1$ for square DE system, 1.22 for circular system

4 Sail Fabrication

While investigating the margin of error in sail fabrication, it is necessary to find the best possible case and then derive deviations away from it. Hence, we investigate both the laser beam and the sail structure and their combinations to obtain the most efficient combination under the given limitations.

4.1 Material

Various materials have been suggested for use in the lightsail for a laser-propelled mission to the Alpha Centauri system.

The use of low near-infrared beams to reduce atmospheric disturbance for a ground-based array requires that the material of the sail would have to be able to reflect such wavelengths of light. These wavelengths would then require a material that reaches a compromise between reflectivity, weight and heat generation.

The current solar reflectors have thickness in the range of 1-10 μm. But future work in this technology is expected to allow us to greatly reduce the thickness of the reflector material and extend the capabilities of our sail.

Additionally, reflectivity has been considered to be unity in all subsequent demonstrated calculations. This has not yet been achieved, though there exist fabricated materials that have close to this value.

Below, we describe some of the reflector technologies in existence today. [1]

1. Multi layer dielectric on metalized plastic film: These systems can achieve reflectivities as high as 99.995% which can be tuned only to a very narrow linewidth. These systems are prone to high levels of error if the linewidth of the laser is wide.

2. Multi layer dielectric on metalized glass: This technology can achieve "the 5 nines" of reflectivity i.e. reflectivities as high as 99.999%. The absorption through this material would be less than 10ppm. This, again, has the limitation of being operational on very narrow linewidths.

It is worth noting here that absorption levels as less as 0.5 ppm have also been achieved but the thickness of the mirrors used would have to be in the order of centimeters which is the reason they would not be suitable in our sail.

Hence, even using existing technology, our assumption of taking ϵ to be 1 is quite reasonable.
Lubin [1] has consistently used a reflector thickness of 1000 nm with a density of 1400 g/m^3. In this paper, we move beyond these limitations, effectively varying both parameters to within reasonable limits of future innovation. Sails as thin as 10 nm with a density in the order of micrograms per square meter have not been established as feasible at this point in time, and so we do not go near these limits while varying our parameters for optimization.

4.2 Correlation of Shape and Stability

For stable flight, the combination of sail shape and laser beam shape play an essential role. At the acceleration the sail experiences, deformation may easily take place. Encountering even minor debris has the potential to send the sail off its path. The laser beam can be multimodal, uniform, or Gaussian, and each of these configurations would interact with individual sail shapes in different ways. Thus, the beam-sail combination should be one that is self-stabilizing to a large extent.

The total force applied by a beam incident on a perfectly reflective sail of area S is given by

$$\frac{\mathrm{d}\vec{F}}{\mathrm{d}t} = \int_S 2\frac{P(x)\vec{b}.\vec{n}(x)}{c}\vec{n}(x)\mathrm{d}S \tag{2}$$

where the domain of integration is the surface of the sail, $\vec{n}(\vec{x})$ is the unit vector normal to the sail surface at the point $\vec{x}$. $P(\vec{x})$ is the beam power flux at the point $\vec{x}$, $\vec{b}$ is a unit vector parallel to the beam axis and c is the speed of light. Similarly, the total torque applied by the beam to the sail is given by

$$\frac{\mathrm{d}\vec{\tau}}{\mathrm{d}t} = \int_S 2\frac{P(x)\vec{b}.\vec{n}(x)}{c}(\vec{r}(\vec{x}) \times \vec{n}(\vec{x}))\mathrm{d}S \tag{3}$$

The sails can be convex, concave or flat. Convex sails would not be able to maintain their structure due to beam pressure. This same pressure would hold up the concave sail by keeping it under tension. If the sail is assumed to be rigid, its motion can be described by Newton's second law, and Euler's equation:

$$I\frac{\mathrm{d}\vec{\omega}}{\mathrm{d}t} + \vec{\omega} \times I\vec{\omega} = \vec{\tau} \tag{4}$$

Three sail shapes were analysed - **spherical, conical and flat** with a flat laser beam with sharp radial profile [6]:

1. **Spherical** :

   (a) Non-collapsible sail - Considering the spherical shape to be rigid, for the craft to be stable, the distance between the centre of mass of the craft and the the vertex of the sail should be more than the diameter of the sail. This requires the payload to be suspended at a large distance from the sail. For stability when the above condition is not fulfilled, the sail needs to be rotated along its axis. This would require an additional torque, which would be difficult to produce.

   (b) Collapsible sail - For a non-rigid sail, at the acceleration which we would subject the it to, the spherical sail would get deformed into an oblate spheroid. This would ruin its symmetry and therefore, its stability. At speeds approaching c, most currently available materials would not hold up to the strain of flight. [8]

2. **Conical** : In this case, a perturbation would take the edge of the sail out of the beam column. Similar to the spherical case, for stability, the distance between the vertex and the centre of mass of the nanocraft should be more than twice the slant height of the cone. For a conical sail, we also have to ensure that multiple reflections do not occur, so angle from horizontal cannot be more than 30 degrees. Simulations at JPL and University of New Mexico [10] showed stability for sail shapes with the conical surface at angles from the horizontal of 25 to 30 degrees, a very small range.

3. **Flat** : A planar sail under uniform illumination (I(x,y)=const) and angle independent reflection (R(v,α)=const) is shown to be unstable

A preliminary conclusion is that the most stable and the simplest sail configuration would be a spherical sail [6], but the suspended chip at such a large distance predicts that a single collision with an external particle may lead to the loss of the associated chip, effectively putting an end to the mission.

Concurrently, two models were suggested, this time using a Gaussian beam. [7] The first one was a rotating conical sail riding on a Gaussian beam. The instability of a conical sail discussed above holds in this scenario, and so we shall not consider this further.

In the second model, a hollow donut-shaped beam was suggested. The hollow beam would consist of 4 Gaussian beams. The payload would be inside a spherical sail, which would remain in the hollow of the beam. This sphere would oscillate, but these oscillations would be restricted to the potential well created by the beam. However, in this model, 80% of the laser energy would be lost. Thus, this model, while allowing stability, loses practicality.
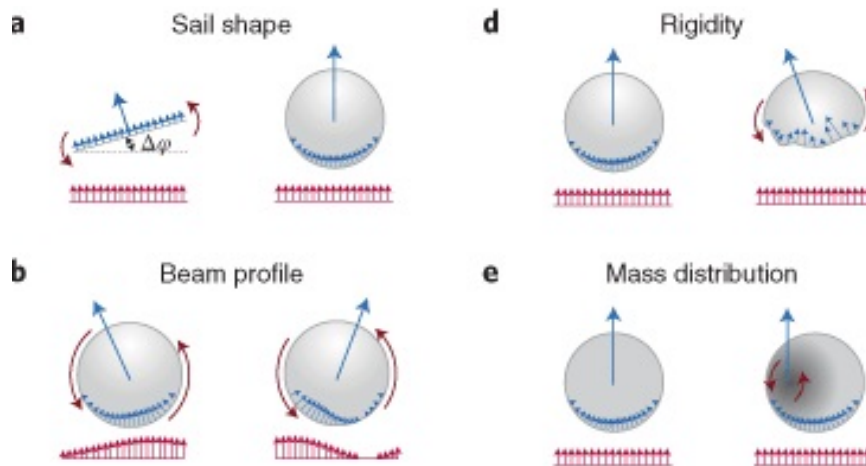
Figure 1: Key design considerations for the stability of a laser propelled spacecraft. [9] Here red arrows denote schematically laser beam illumination, blue arrows correspond to local and total laser induced forces.

5 Physics of Laser Propulsion

Working towards a comprehensive solution, a non-relativistic case is presented and then extended to a relativistic frame.

While a discussion on the optimal beam shape and sail configuration combination with regards to stability has already been detailed above, the simplest case to computationally analyze and compare across both frames under the limitations that the

- craft's terminal velocity approaches 0.2c
- surface area of the craft is 10 square meters
- laser array power is 50GW
- sail material is (as explained above) within reasonable limits of future innovation

is that of the square sail propelled using a uniform beam.

As a result, the stability is approached independently of the subsequent analysis of dynamics of the square sail propelled on a uniform beam. During analysis of dynamics it is assumed that the craft remains stable and is undeviated from its intended path.

5.1 Non-Relativistic Case

Carrying out an analysis as given in [1]:

Laser thrust on payload with laser power P_0 with reflectivity ϵ_r while laser spot is smaller than sail

$$F = \frac{P_0(1 + \epsilon_r)}{c} \tag{5}$$

where ϵ_r=0 for no reflection (all absorbed) and 1 for complete reflection. For our purpose, ϵ_r 1

Acceleration

$$a = \frac{F}{m} = \frac{P_0(1 + \epsilon_r)}{mc} \tag{6}$$

Total mass = base payload + total mass of sail

$$m = m_0 + m_{sail} \tag{7}$$

$$m_{sail} = D^2 h\rho \tag{8}$$

where D=sail size, h=sail thickness, ρ=sail density

$$D(m) = \sqrt{\frac{m_{sail}}{h\rho}} = 31.6\sqrt{\frac{m_{sail}(kg)}{h(\mu)\rho(g/cc)}} \tag{9}$$

Speed at point where laser spot = sail size

$$v_0 = \left(\frac{P_0(1+\epsilon_r)dD}{c\lambda(D^2h\rho+m)}\right)^{1/2} \tag{10}$$

Distance L_0 at which laser spot = sail size

$$L_0 = \frac{Dd}{2\lambda} \tag{11}$$

The time taken to where the laser spot equals the sail size is:

$$t_0 = \left(\frac{cdD(D^2h\rho+m)}{P_0(1+\epsilon_r)\lambda}\right)^{1/2} \tag{12}$$

After this point, the force is no longer constant. The laser beam does not fall completely on the sail but some portion of the beam overflows from the sail; this power is essentially lost.
With continued illumination, the speed increases by $\sqrt{2}$

$$v_\infty = \left(\frac{2P_0(1+\epsilon_r)dD}{c\lambda(D^2h\rho+m)}\right)^{1/2} \tag{13}$$

It can be shown that the maximum speed occurs when the sail mass = the payload mass

5.2 Relativistic Case

In this approach [2], initially it is observed that the momentum of the photons and the nanocraft, is conserved before and after the collision. This is a simple Compton scattering phenomena. Considering that the source of the laser (Directive energy system) is stationary, and the energy of a single photon is small compared to the rest energy of the sail, the individual collisions can be smoothed over.
Due to relative motion between the sail and DE system, the rate at which the

photons are emitted from the system is not the same as the rate at which they strike the sail.

$$E_f = \left(\frac{1-\beta}{1+\beta}\right) E_i \tag{14}$$

(due to 2 Doppler shift factors)
E_i is initial energy of photons
E_f is energy after reflection from sail

Rate of change of $\beta =$

$$\dot{\beta} = \frac{2P}{mc^2\gamma^3}\left(\frac{1-\beta}{1+\beta}\right) \tag{15}$$

As photons reflect off the sail, they get redshifted, transferring their energy to the sail. The efficiency of a collision can be defined as the fraction of energy transferred at each collision.

$$\eta = \frac{\Delta E}{E_i} = \frac{2\beta}{1+\beta} \tag{16}$$

As the speed of the sail increases, the photons take longer to strike the sail. Thus, more of the energy from the DE system is used in the forward photon beam rather than in acceleration of the sail.
For distance greater than L_0, power reduces with distance according to the inverse square law. Thus, an equilibrium is established and a terminal velocity is reached.

Observing the nanocraft in the relativistic frame has thus allowed us to conclude that it reaches its terminal velocity within the mandated timeframe of 20 minutes.

The relevant conclusion we can derive from this graph is that the sails with smaller mass reach their terminal velocity faster than the larger masses because of greater acceleration. Also, they have a larger terminal velocity than the heavier sails.
Additionally, we observe that the 1 km DE system has more divergence than the 10km one. L_0 is smaller for the 1km system, thus, the time taken for them to reach terminal velocity is smaller than for the other one. The terminal velocity is lesser for the sail accelerated by 1km system.
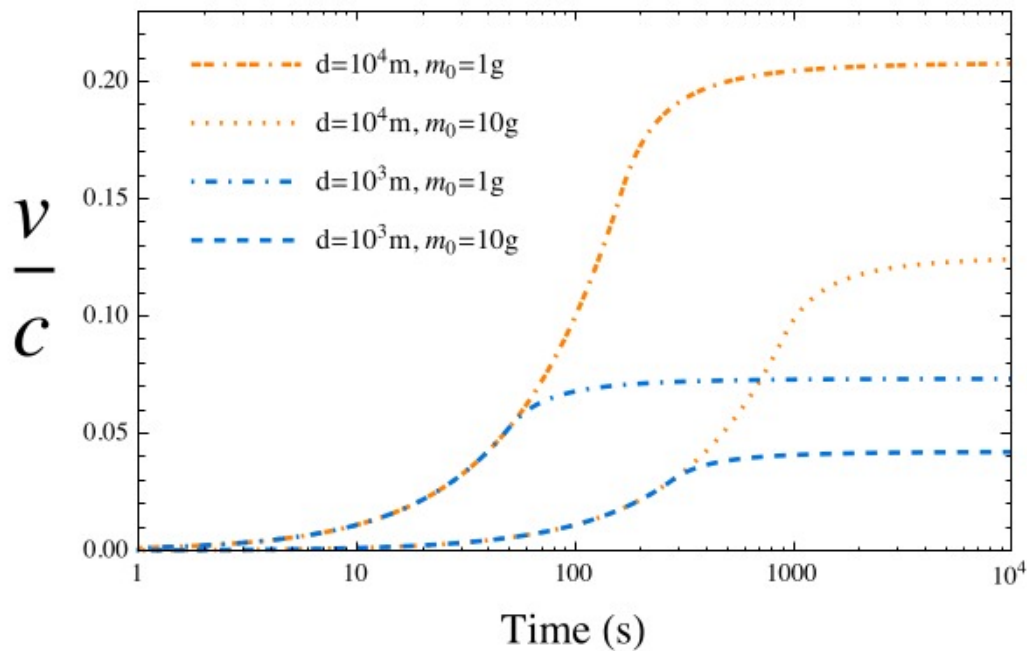
Figure 2: Taken from [2], this graph shows the implications of a relativistic frame

5.3 Differing Sail Dynamics for Uniform Beam

Above, we have observed the difference of the relativstic and non-relativistic frames. These calculations have all been done using a square laser array and a square sail shape combination. We now obtain data from [3] keeping in mind the limitations of the problem and the intended voyage, and observe the difference between the two frames to showcase the importance of the extension.

From the graph in figure two it is visible that the payload at which the limiting parameters allow us to approach 0.2c is 2 grams. At this low mass, the increased deviation of the relativistic case from the non-relativistic case is also seen.
We now move away from a square laser array to a circular one. The use of a circular array allows the comparison of different sail shapes for the same payload. This also becomes a factor in choosing a sail for optimum performance.

On comparison of the different sail shapes for the same circular laser array, the incremental benefit of using the circular sail for this configuration becomes visible. However, we do not yet know whether the circular sail's performance for a circular laser array is better than that of a square sail of the same area for a comparable square array.
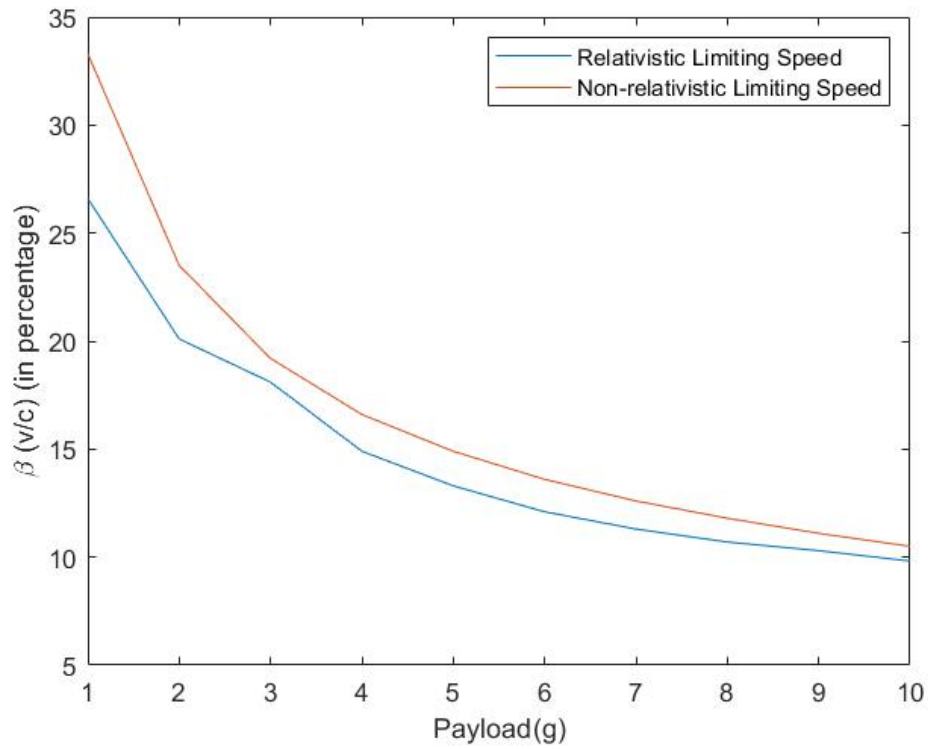
11

Figure 3: Variation of the limiting speed for a square sail propelled by a square DE-STAR 4 laser array of 50 GW for differing payloads. The surface area of the craft has been kept constant at 10 square meters in accordance with the problem statement.

This question is addressed in the next graph, by plotting their relative performances side by side.
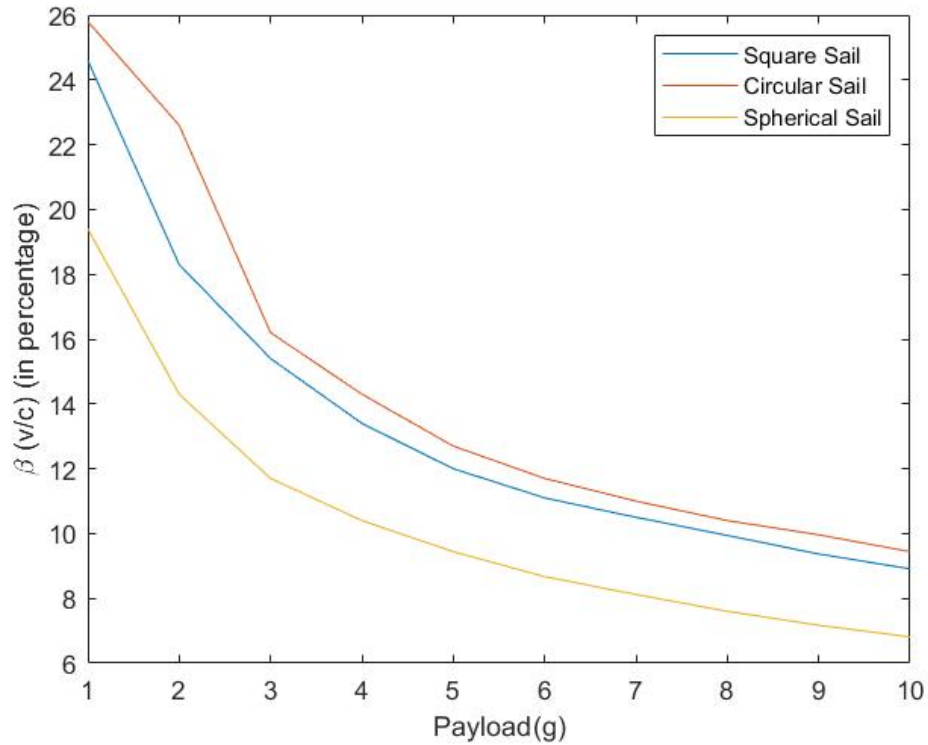
Figure 4: Variation of the limiting speed for different sail shapes in the relativistic frame propelled by a circular DE-STAR 4 laser array of 50 GW for differing payloads. The surface area of the craft has been kept constant at 10 square meters while varying the areal density.

6   Acceleration Dynamics

On viewing the graphs we can take the highest mass to achieve close to 0.2c as 2g. We can now calculate the constants derived under the non-relativistic frame.This gives us the values

$$L_0 = 1.49 * 10^7 km$$

$$t_0 = 9.97 minutes$$

$$v_0 = 4.99 * 10^7$$

$$\beta_0 = 0.166$$

We are illuminating the sail for 20 minutes and during that acceleration, our sail speed reaches close to its maximum speed on continued illumination beyond
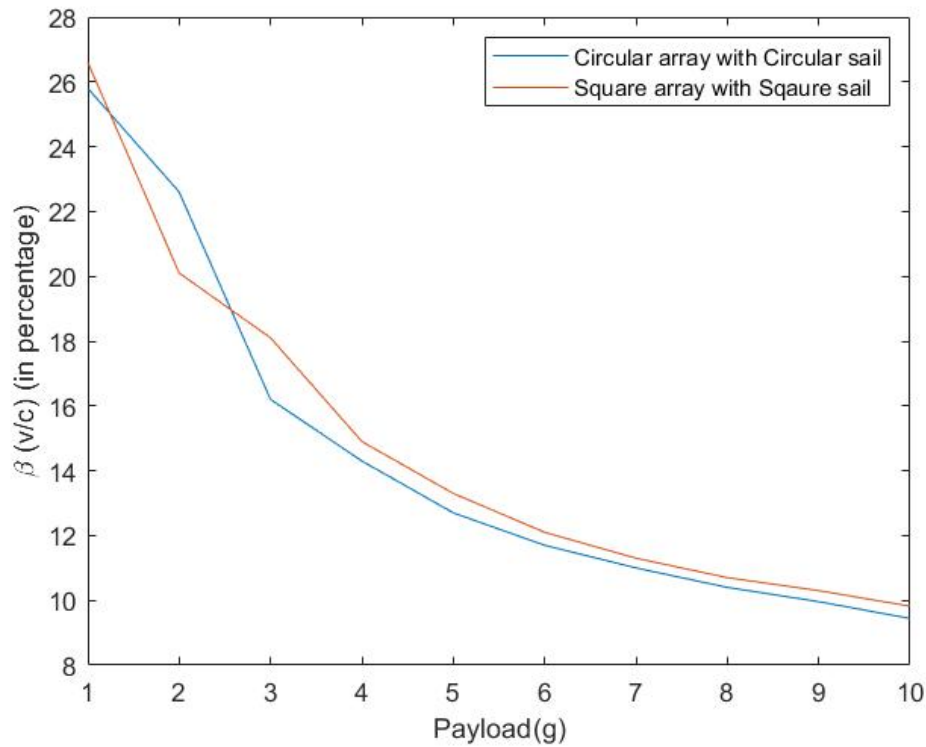
Figure 5: A plot of the two better performing sail shapes to clarify the relationship between array shape and sail shape

t_0, as proved in our analysis above.

The laser is switched on only for the first 20 minutes and then switched off. We operate under the assumption that the nanocraft is stable on the beam (an assumption which has been discussed in early sections), and that the nanocraft will travel undeviated by external gravitational fields until it reaches the vicinity of Proxima Centauri. This is a reasonable assumption to make as Proxima Centauri B is the closest known exoplanet to Earth and Proxima Centauri is the nearest star, mitigating the possibility of interference by other astronomical objects.

Basis for disregarding the Sun's gravitational field in comparison to laser acceleration:

Gravitational force of Sun: 0.00002 N
Force due to laser: 333.33 N

Thus the gravitational force of the sun is seven orders of magnitude less than the force given to the lightcraft by the laser, and will also decrease further according to the inverse square law as the lightsail moves away from the elliptic plane. Hence it is disregarded.

The acceleration dynamics thus effectively reduce to the problem of choosing the right time and initial nanocraft positioning in orbit such that a linear impulse given by the laser photons will send it directly in the direction of the Proxima Centauri system.

7   Laser Precision

There is sparse data on the inclination of the elliptic plane of orbit of the Proxima Centauri System, perhaps due to the relatively recent discovery of the terrestrial-like planet from the analysis of Doppler measurements in 2016. Under the assumption that the lightcraft will first come in the vicinity of the exoplanet before passing closer to the star.

We know that:
Distance from earth to proxima centauri = 4.105 x 10^{13} km
Earth moon distance = 384,400 km
Radius of expoplanet = 0.8-1.5 R_e = 5096-9557 km
Proxima B orbits the star at 7.5 x 10^6 km
In order to pass at a distance less than 384,400 km to Proxima Centauri b, the maximum allowable half deviation angle of the laser from its optimum value (with the origin line directed at the expolanet) is

$$\theta_{\text{dev}} = \frac{3.844 \times 10^5}{4.105 \times 10^{13}} = 9.364 \times 10^{-9} \tag{17}$$

If the laser array provides with any lesser precision, the nanocraft will pass outside of the mandated required flyby distance.
In order to further optimize the stability of the path, we also limit the precision of the laser such that the laser beam cannot deviate to an extent more than that which takes the centre of the beam outside the spectral area of the nanocraft on a non-deviated path until the craft is at a distance L_o (which has been calculated above)

$$\theta = \frac{D/2}{L_o} = 1.061167 \times 10^{-10} \tag{18}$$

15

If the laser is constructed in line with the more stringent parameter of the order of -10 above, it effectively ensures that the spacecraft will reach the intended destination.

We also calculate the angle of divergence of the laser beam itself.

$$\theta = \frac{\lambda}{d} = \frac{1.064 \times 10^{-6}}{10^7} = 1.064 \times 10^{-13} \tag{19}$$

This shows that the spreading of the laser beam, assuming that the laser points exactly where we want it to, will take the nanocraft well within the mandated distance for a flyby. However, deviations and disturbances in the direction of the laser beam itself need to be accounted for separately, as has been done above.

8   Conclusions

The square sail, by pure parametric analysis during externally stabilized motion on a uniform beam, is arguably the best choice among those examined. However, when examining solely stability of the setup while disregarding the parameters of power efficiency and material strength, it becomes apparent that the spherical sail using a multimodal Gaussian beam is optimum.

However, in reality the spherical sail, whose thickness is in the order of microns, would become ablated at high relativistic speeds. Another geometry considered, conical, is not fit to use due the trade-off it needs to make between the efficiency of the laser beam incident on it and the stability of the sail.

Another thing to note is that this work does not take into account the rotation of the earth over these 20 minutes due to which the laser fixed on the ground would also deviate from pushing the sail exactly from its centre and thus providing a torque which could throw the probe off its required path.

Further examining the square sail, we have shown its margin of improvement for differing payloads as opposed to circular and spherical sails for a perfectly uniform laser beam (further clarified in the appendix below). But there are still various problems with that geometry which we have ignored during our analysis of dynamics, prominent among which is the stability of such a system, which our prior analysis has shown to be low.

The precision of the laser system has been examined with the maximum angle deviation being 1.06×10^{-10} radians in the two-dimensional plane. Beam divergence has also been examined.

There is still a significant amount of work required to solve the problem of stability of probe sail, laser precision, and the best material to make the sail out of before such a spacecraft could be invested in and sent on expeditions. The parameter space to be explored is huge and to pick out the optimum values from that space is one of the largest obstacles to overcome. To make even better optimizations of the parameters associated and achieve them with the required precision in real life using large computational power is absolutely essential to completing the proposed journey spanning decades.

Further extension of this work and more innovation is required to think of a mission to land the spacecraft onto bodies of the likes of Proxima Centauri b in addtion to performing flybys. The prominent difficulty in landing such nanocraft is the means to decelerate a spacecraft that barely carries anything but the sail which drives it. For now, this spacecraft is a promising idea to venture into places unreachable before.

References

[1] P. Lubin. A Roadmap to Interstellar Flight. *JBIS*, Vol. 69, pp. 40–72, 2016

[2] N. Kulkarni, P. Lubin, Q. Zhang. Relativistic Spacecraft Propelled by Directed Energy. *Proc. SPIE 9981*, Planetary Defense and Space Environment Applications, 2016.

[3] unknown, University of California Santa Barbara Laser Propulsion. `http://www.deepspace.ucsb.edu/wp-content/uploads/2015/04/Relativistic-Laser-Propulsion-Classical-1D-Standalone.html`.

[4] K. L. G. Parkin. The Breakthrough Starshot System Model, Acta Astronaut

[5] R. L. Forward. Roundtrip interstellar travel using laser-pushed lightsails, *Journal of Spacecraft and Rockets* 21(2), pp. 187–195, 1984

[6] H. Popova, M. Efendiev, I. Gabitov, On the stability of a space vehicle riding on an intense laser beam `https://arxiv.org/abs/1610.08043` (2016)

[7] Z. Manchester, A. Loeb, *Astrophys. J.* 837, L20 (2017)

[8] P. Gilster, 2017, `www.centauri-dreams.org/2017/06/23/beam-riding-and-sail-stability`

[9] H. A. Atwater, A. R. Davoyan, O. Ilic, D. Jariwala, M. C. Sherrott, C. M. Went., W. S. Whitney, J. Wong, Materials challenges for the Starshot lightsail. Nat. Mater. 2018, DOI: 10.1038/s41563-018- 0075-8.

[10] G. Benford, O. Goronostavea and J. Benford, Experimental Tests Of Beam-Riding Sail Dynamics, Beamed Energy Propulsion, *AIP Conf. Proc.* 664, pp. 325, A. Pakhomov, ed., 2003

Appendix

Table 1: Relativistic vs. Non-relativisitic limiting speeds varying with payload mass (with square laser array)

Payload(g)	$\beta\%$(Relativistic)	$\beta\%$(Non-Relativistic)
1	26.6	33.3
2	20.1	23.5
3	18.1	19.2
4	14.9	16.6
5	13.3	14.9
6	12.1	13.6
7	11.3	12.6
8	10.7	11.8
9	10.3	11.1
10	9.82	10.5

Table 2: Relativistic Limiting Speeds for sails of different geometries(with circular laser array)

Payload(g)	$\beta\%$(Square)	$\beta\%$(Circular)	$\beta\%$(Spherical)
1	24.6	25.8	19.4
2	18.3	22.6	14.3
3	15.4	16.2	11.7
4	13.4	14.3	10.4
5	12	12.7	9.44
6	11.1	11.7	8.67
7	10.5	11	8.12
8	9.94	10.4	7.6
9	9.37	9.96	7.17
10	8.91	9.44	6.81